Oblique impact of a buckling table-tennis ball on a rigid surface

Théophile Rémond, Vincent Dolique, Renaud G Rinaldi, Jean-Christophe Géminard

Featured in Physics

Oblique impact of a buckling table-tennis ball on a rigid surface

Théophile Rémond,[1] Vincent Dolique,[1] Renaud G. Rinaldi,[2] and Jean-Christophe Géminard[1]
[1]*LPENSL, CNRS UMR5672, ENS de Lyon, Université de Lyon, F-69342 Lyon, France*
[2]*MATEIS, CNRS UMR 5521, INSA-Lyon, Université de Lyon, F-69621 Villeurbanne, France*

(Received 19 December 2022; accepted 17 April 2023; published 26 May 2023)

We report on the rebound of a table-tennis ball impinging without any initial spin in oblique incidence on a rigid surface. We show that, below a critical incidence angle, the ball rolls without sliding when bouncing back from the surface. In that case, the reflected angular velocity acquired by the ball can be predicted without any knowledge of the properties of the contact between the ball and the solid surface. Beyond the critical incidence angle, the condition of rolling without sliding is not reached within the time of contact with the surface. In this second case, one can predict the reflected angular and linear velocities, as well as the rebound angle, provided the supplementary knowledge of the friction coefficient associated with the ball-substrate contact.

DOI: 10.1103/PhysRevE.107.055007

I. INTRODUCTION

In most ball games, there are rebounds of the ball on some surfaces, which can be of different kinds. Ultimately, a better understanding of the interaction between the ball and the substrate can be significant for the players, especially of the rotational speed of the ball after rebound, as it will influence the way they will control it and therefore adjust to it. In table tennis for instance, the less the ball rotates, the better the player can attack with a suitable stroke.

Many authors studied the rebound of a ball in oblique incidence, mostly without initial spin [1–4]. From a purely theoretical point of view, if one considers a perfectly rigid ball during the impact, the ball will start rolling if the friction force is large enough, independently of the mass and size of the ball. Otherwise, the ball will slide and the rebound properties are determined by both the coefficient of friction and the coefficient of restitution of the normal velocity. These equations are detailed by Brody [1]. It is worth mentioning that this theory neglects the elastic deformation of the solid bodies. Maw *et al.* developed a numerical model which extends the Hertz contact theory, dividing the contact surface into concentric annuli among which some are slipping and some are sticking to the surface. The result is that the friction force reverses during the rebound, allowing the ball to spin faster than what is predicted by the rolling condition [5]. This model has been validated experimentally when studying a solid perfectly elastic ball on a similar surface [6–9].

There are very few studies about the rebound of hollow spheres, which are inelastic, on a perfectly elastic surface in oblique incidence. One can wonder which model has to be taken into account when considering the fact that only the ball will deform. Cross studied the behavior of tennis balls on different surfaces and showed that the ball only rolls on a high friction coefficient surface, at a high incident angle of 45° from the surface [2]. Additionally, he came to the conclusion that bouncing balls, including tennis balls, do not roll [3]. Furthermore, most of the studies presented above are performed at low incident linear velocities, around 3–4 m s^{-1}.

Yet, a thin-walled sphere is known to buckle past a critical velocity, which depends on the shell thickness and material properties [10]. The buckling of the shell might have significant consequences on the rotation of the ball after rebound. The present paper investigates the rebound of a table-tennis ball impacting onto a tilted rigid surface, within a large range of incident linear velocities (from 2 to 13 m s^{-1}). For such a ball, the typical velocity leading to buckling is around 6 m s^{-1}. We show that the behavior of the ball can be completely described by Brody's theory and that the buckling instability does not alter the final motion of the ball.

II. EXPERIMENTAL PRINCIPLE AND SETUP

The aim of the experiment is to study the rebound of a table-tennis ball without incident spin in oblique incidence. For practical reasons, we consider the rebound of a ball traveling downwards vertically impinging on an inclined solid surface as depicted in Fig. 1. The angle of incidence θ_i is defined to be the angle between the incident velocity $\vec{v}_i$ and the normal to the surface oriented downwards $\overrightarrow{CP}$, i.e., $\theta_i = (\vec{v}_i, \overrightarrow{CP})$. It is oriented so that it equals the tilt angle α of the surface.

Due to the action of the contact force $\vec{F}$ during the collision, the ball starts spinning. It leaves the surface with the reflected velocity $\vec{v}_r$ and rotates with the angular velocity $\vec{\omega}_r$ around the out-of-plane x axis. For convenience, we denote θ_r the reflected angle that the velocity $\vec{v}_r$ makes with the normal to the surface oriented upwards $\overrightarrow{PC}$, i.e., $\theta_r = (\overrightarrow{PC}, \vec{v}_r)$. With this choice, we have $\theta_r = \theta_i$ if the tangential component of the incident velocity is conserved after the rebound and its normal component changes in sign only.

The experimental setup is designed to measure $\vec{v}_r$, θ_r, and $\vec{\omega}_r$ as a function of the incidence angle θ_i and impact velocity $\vec{v}_i$. The ball [Cornilleau™, P-ball 3 stars, 4 cm in diameter, mass 2.7 g, acrylonitrile butadiene styrene (ABS) plastic] is launched with the velocity $\vec{v}_i$ vertically owing to a home-made impactor already described elsewhere (see Ref. [10]). It

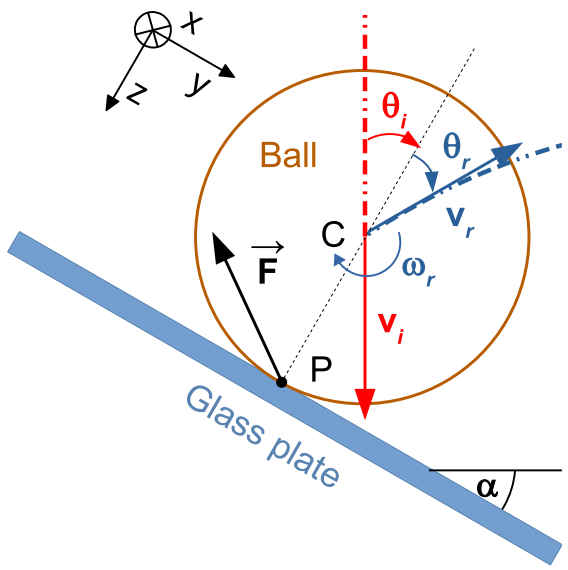

FIG. 1. Metrics for the vertical impact of a ball on a titled rigid surface. The ball reaches the solid surface with the vertical velocity $\vec{v}_i$ without initial spin. The surface is tilted by the angle α. After rebound, due to the action of the contact force $\vec{F}$ during the collision, the ball spins with the angular velocity $\vec{\omega}_r$ and the reflected velocity of the ball $\vec{v}_r$ makes the angle θ_r with the normal to the surface.

consists of a metal rod initially armed by compressing a spring. The ball is then put into place in a holder underneath. The striker is subsequently released. The ball reaches the solid surface, a firmly held 2.8-mm-thick transparent glass plate, with a vertical incident velocity v_i, which is tuned to vary from 1 to 13 m s^{-1} depending on the initial compression of the spring.

The rebound of the ball is observed from one side with a high-speed camera (Fig. 2). The optical axis of the camera (Kron Technologies, Chronos 2.1-HD, monochrome image sensor, 2142 fps) is along the normal of the incidence plane (x axis) to keep the whole rebound in the same focal plane.

For each test, the incidence angle θ_i is set owing to a pivot connection on the metallic structure holding the glass plate. In addition, the ball joint located on the equator is marked in order to ensure the same initial orientation of the ball from one test to another (noting that the joint exhibits a greater thickness resulting in a local enhanced stiffness which is likely to alter the impact response). The incident angle as well as the relevant characteristics of the rebound are determined on the recorded images using the image analysis software IMAGEJ [11]. The velocities of the ball before and after it comes in contact with the surface are measured as a function of time t to account for the acceleration due to gravity. Then, by interpolation, the velocities right before, v_i, and right after, v_r, the contact are evaluated at the collision time, defined as the time when both trajectories, before and after the rebound, intersect. The rebound angle θ_r is calculated by interpolating the trajectory in space of the center of the ball to a polynomial of order 2. Finally, ω_r is evaluated considering the rotation of the dashed line drawn on top of the ball equator (i.e., the joint).

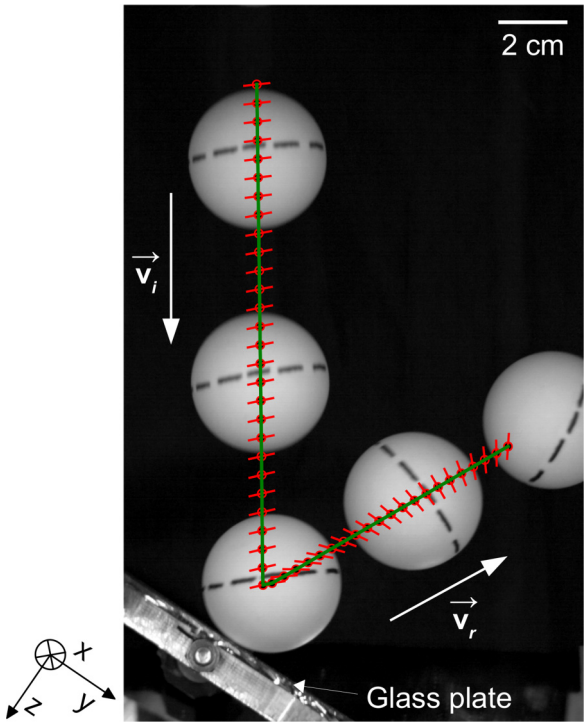

FIG. 2. Superimposition of five images of the ball around the collision with the tilted glass window and associated trajectory. Only five images separated by a time difference of 5.6 ms are displayed here. The black dashed line drawn on the ball allows identifying the ball joint and is used for the determination of the ball angular velocity. For each image of the movie (frame rate: 2142 fps), we determine the position of the center of the ball (red circle) and the angular position of the ball (red dashed). From the successive positions of the center we obtain the incidence angle $\theta_i = 35^\circ$ and the incident velocity $v_i = 11.6$ m s^{-1}. From the successive angular positions of the ball we get the angular velocity $\omega_r = 190$ rad s^{-1}.

III. RESULTS

A. Experimental results

In Fig. 3(a), we report the angular velocity ω_r as a function of the incidence angle θ_i for various incident velocities v_i. We observe that, as intuitively expected, ω_r increases from zero as the incidence angle θ_i is increased (noting that $\theta_i = 0$ corresponds to the normal incidence). However, when the glass window is tilted further, i.e., when the incidence angle exceeds typically 45°, the angular velocity ω_r is seen to drop with a further increase of θ_i. It is of particular interest to note that below typically 45° and for the range of initial velocities covered, the angular velocity ω_r is simply proportional to the incident tangential velocity $v_{y,i} = v_i \sin(\theta_i)$ as can be observed in Fig. 3(b).

In addition, when displaying the restitution coefficient associated with the normal component of the velocity, $\varepsilon_z = -v_{z,r}/v_{z,i}$ as a function of $v_{z,i}$, for various values of the incident velocity v_i and incidence angle θ_i, one observes a great collapse of the data (Fig. 4). The restitution coefficient ε_z does not seem to depend on the incidence angle, i.e., on the tangential component of the velocity $v_{y,i}$. We thus observe a clear independence of the dynamics along the normal which

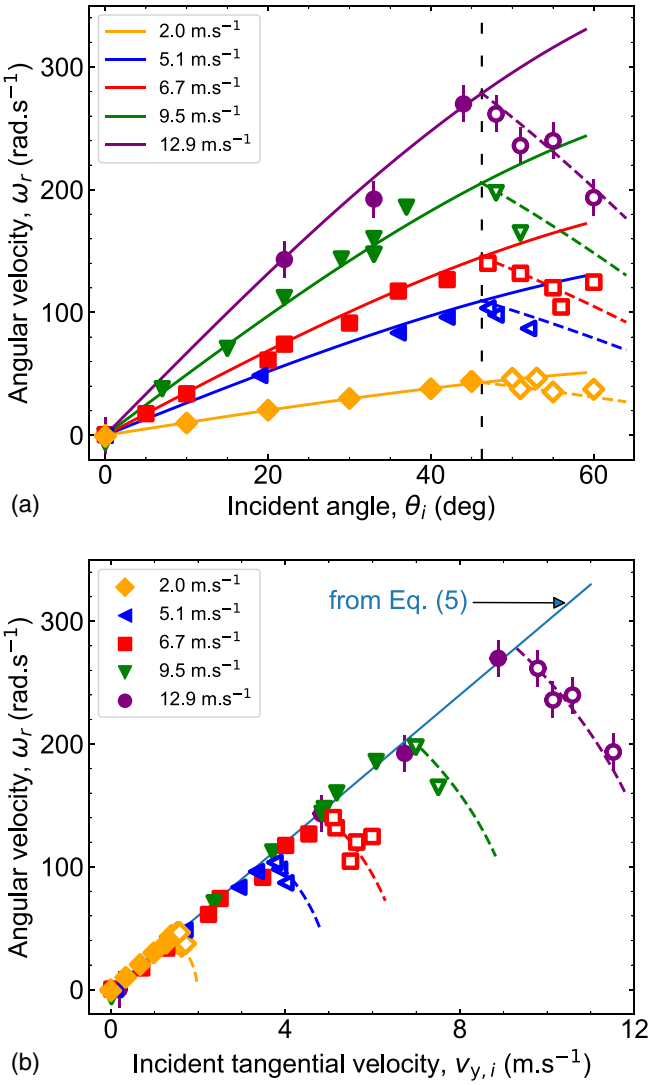

FIG. 3. Angular velocity ω_r vs (a) incidence angle θ_i and (b) incident tangential velocity $v_{y,i}$. In (a), one observes two regimes. For angles θ_i typically below 45°, ω_r increased when θ_i is increased. By contrast, beyond typically 45° the angular velocity ω_r drops down. In (b), one observes that below the transition, ω_r is simply proportional to $v_{y,i}$, regardless of the norm of the incident velocity v_i. In (a) and (b), the solid lines are the prediction of Eq. (5) which assumes that the spherical shell is rolling without sliding when it leaves the solid surface and the dotted lines are the prediction of Eq. (8) which assumes that the spherical shell is still sliding when it leaves the solid surface ($\varepsilon_z = 0.9$ and $\mu = 0.22$).

can thereafter be considered independently. Moreover, as already evidenced in the case of normal incidence impact, ε_z exhibits two regimes on both sides of a critical incident normal velocity $v^c_{z,i} = (7.5 \pm 0.5)$ m s^{-1}. It has been shown that for impacts with incident normal velocities greater than $v^c_{z,i}$ the spherical shell of the ball is subjected to an elastic buckling instability [10].

In what follows, we show how straightforward mechanical arguments account for both the proportionality between ω_r and $v_{y,i}$ and the critical incidence angle θ^c_i beyond which the linearity ceases to apply.

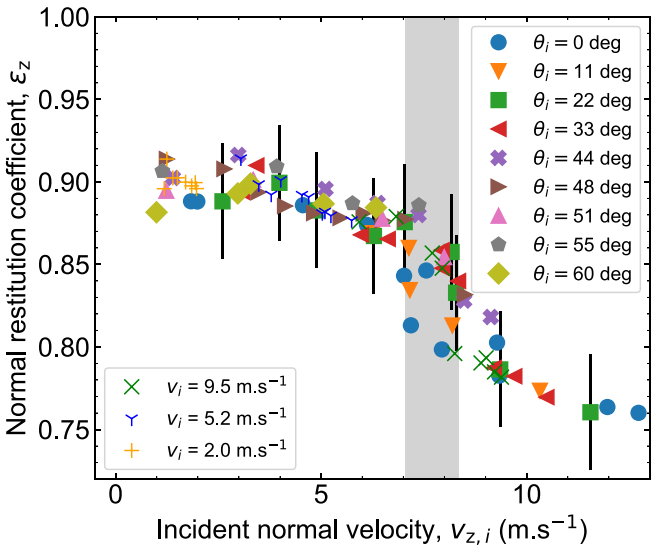

FIG. 4. Restitution coefficient of normal velocity ε_z vs normal velocity $v_{z,i}$. The collapse of the data in a single trend shows that the restitution of the normal component of the velocity is not altered by the tangential component. The gray vertical region highlights the transition to the buckling instability which occurs within the vicinity of the critical velocity $v^c_{z,i} = (7.5 \pm 0.5)$ m s^{-1}.

B. Small incidence angle $\theta_i < \theta^c_i$

As previously shown, for moderate incidence angles, $0 < \theta_i \leqslant \theta^c_i$, the reflected angular velocity ω_r is observed to be proportional to the tangential component of the incident velocity $v_{y,i}$, independent of the magnitude of the incident velocity v_i.

In order to understand this experimental fact, one can consider for the sake of simplicity, that a spherical shell of mass m and moment of inertia J comes into contact with a solid substrate and that none of the solids deforms during the collision. During the contact time τ, the substrate exerts a force $\vec{F}$ (which depends on time) on the shell. Denoting $\vec{v}_i$ and $\vec{v}_r$ the impact velocity before and after the rebound, respectively, one can write from the fundamental principles of the dynamics

$$m(\vec{v}_r - \vec{v}_i) = \int_0^\tau (\vec{F} + m\,\vec{g})dt, \tag{1}$$

$$J(\vec{\omega}_r - \vec{\omega}_i) = \int_0^\tau (\overrightarrow{CP} \wedge \vec{F})dt, \tag{2}$$

where C and P denote the center of the spherical shell and the point of contact, respectively. The origin of time is taken to coincide with the onset of the contact. We remind here that the incident angular velocity $\vec{\omega}_i = \vec{0}$. We note that in Eq. (1), the rigid shell is subjected to the acceleration due to the gravity $\vec{g}$. However, during the short time of the collision but mostly due to the intensity of the force $\vec{F}$, its effect can be neglected. Noting further that $\overrightarrow{CP} = R\,\vec{z}$ is perpendicular to the solid surface, we can write $\overrightarrow{CP} \wedge \vec{F} = -(R\,F_y)\,\vec{x}$, where F_y is the tangential component of the force $\vec{F}$. The dynamical Eq. (2)

can then be rewritten in projection along the x axis:

$$J\,\omega_r = -R\int_0^\tau F_y\,dt. \tag{3}$$

From Eq. (1), one can write along the y axis

$$m(v_{y,r} - v_{y,i}) = \int_0^\tau F_y\,dt = -\frac{J\,\omega_r}{R}. \tag{4}$$

This relation between the variation of the tangential velocity and the angular velocity holds true as long as the normal component of the force $\vec{F}$ does not apply any torque.

We now assume that, due to the action of the force $\vec{F}$, the spherical shell is rolling without sliding when leaving the surface. This leads to the relation $R\,\omega_r = v_{y,r}$. Using Eq. (4) and the value of the moment of inertia for a spherical shell $J = \frac{2}{3}m\,R^2$, we get

$$R\,\omega_r = \tfrac{3}{5}v_{y,i}. \tag{5}$$

The reflected angular velocity is here proportional to the tangential component of the incident velocity $v_{y,i}$, independent of the magnitude of the incident velocity v_i. The solid line in Fig. 3(b) comes from the theoretical relation in Eq. (5), and is found to fit nicely the experimental data. With $v_{y,i} = v_i\sin(\theta_i)$, one can then interpolate the data reported as a function of the incidence angle in Fig. 3(a). The most striking result obtained from the simple modeling is that the relation does not depend on any experimental parameter except that the ball is a thin spherical shell, which triggers the value of the moment of inertia and thus the 3/5 constant in Eq. (5).

To go further, we remark that $v_{y,r} = \frac{3}{5}v_{y,i}$ enables the estimate of the reflected angle θ_r. Indeed, $\tan(\theta_r) = -v_{y,r}/v_{z,r}$. Denoting ε_z the velocity restitution along the normal to the surface, $\varepsilon_z = -v_{z,r}/v_{z,i}$, we get

$$\tan(\theta_r) = \frac{3}{5\,\varepsilon_z}\tan(\theta_i). \tag{6}$$

In practice, due to the fact that the normal velocity is almost conserved in magnitude (a loss of about 10%) but the tangential velocity is reduced by 2/5 (40%), the trajectory after rebound rears up, and the angle θ_r is smaller than θ_i ($\theta_r - \theta_i < 0$). The latter result depends on the value of ε_z. However, we observe in Fig. 4 that ε_z is almost independent of the incident velocity $v_{z,i}$. Assuming that ε_z is constant, limiting the interpolation to the smallest impact velocities ($v_i < 7$ m s^{-1}) for $\theta_i < \theta_i^c$, we obtain an excellent agreement between Eq. (6) and the experimental data in Fig. 5 for $\varepsilon_z = 0.9$ (least-squares method). This value is compatible with the data displayed in Fig. 4 for moderate incident normal velocity $v_{z,i}$. In addition, we remark that the experimental data are above the trend (green triangles in Fig. 5) for the largest incident normal velocity ($v_{z,i} = 9.5$ m s^{-1}). This observation is also in agreement with Eq. (6) which predicts an increase of θ_r when the incident normal velocity is increased due to the associated decrease of the restitution coefficient ε_z.

C. Critical incidence angle θ_i^c

The theoretical results of the previous section have been obtained assuming that the spherical shell is rolling without sliding when leaving the solid substrate after impact. However, for a prescribed incident velocity, an increase in the incidence angle θ_i causes simultaneously the increase of the tangential velocity and the decrease of the normal one. As a consequence, if, for instance, the tangential component of the force $\vec{F}$ is due to solid friction, it will be less and less able to stop the initial sliding of the contact.

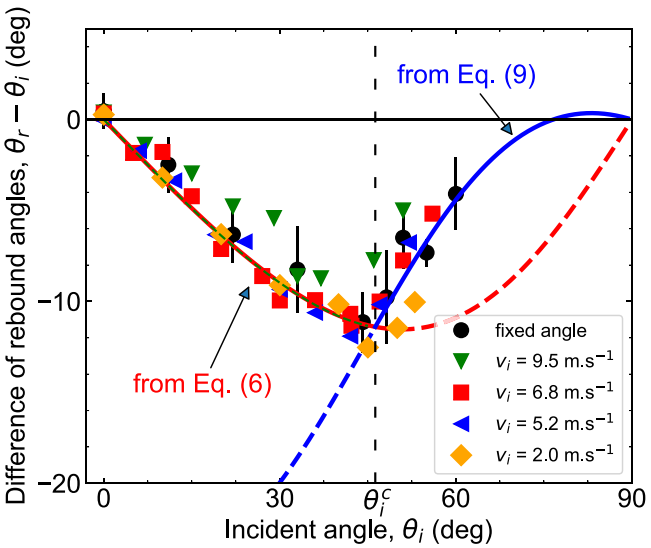

FIG. 5. (a) Difference $\theta_r - \theta_i$ vs angle of incidence θ_i. We observe, for θ_i below 45°, an excellent agreement between the experimental data and Eq. (6) with $\varepsilon_z = 0.9$. Beyond the onset (dotted vertical line), an excellent agreement is observed with Eq. (9) ($\varepsilon_z = 0.9$ and $\mu = 0.22$).

In order to prove that the transition between the two regimes is due to the inability of the system to ensure the conditions of rolling without sliding, we report in Fig. 6 the ratio η of the experimental $R\,\omega_r$ to $v_{y,r}$ which equals 1 in the case of no sliding and 0 for perfect sliding. We observe that the latter quantity equals 1 for θ_i smaller than 45° approximately and decreases drastically when θ_i is higher. The transition is thus clearly due to the fact that the contact point is still sliding when the ball leaves the surface.

In order to account for the transition, yet in a simplistic manner, we consider that the tangential component of the force F_y is due to friction and we simply write $F_y = -\mu|F_z|$ (provided that $v_y > 0$). Considering the dynamics along the normal to the substrate, we have, at all times, $F_z = m\,\dot{v}_z$ (where the overdot denotes the derivative with respect to time). Considering the dynamics in the substrate plane, we have $m\,\dot{v}_y = F_y = -\mu|F_z|$ because the contact point slides during the whole contact time, such that integrated over time $v_{y,r} - v_{y,i} = \mu\,(v_{z,r} - v_{z,i})$. Introducing the restitution coefficient ε_z and the incidence angle θ_i ($v_{z,i} = v_i\cos\theta_i$ and $v_{y,i} = v_i\sin\theta_i$), taking into account that the rolling conditions $v_{y,r} = \frac{3}{5}v_{y,i}$ are still valid at the onset, we get the critical angle θ_i^c in the form

$$\tan\theta_i^c = 5\frac{1+\varepsilon_z}{2}\mu. \tag{7}$$

From the experimental value of $\theta_i^c \simeq 45°$, taking into account that ε_z is close to 1, we get a first estimate of the

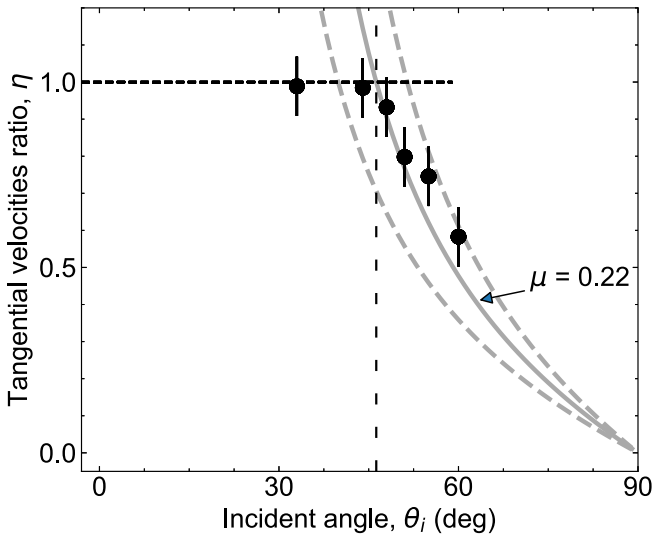

FIG. 6. (a) Ratio $\eta \equiv R\,\omega_r/v_{y,r}$ vs incidence angle θ_i. The experimental data (black disks) are averages over six impact velocities in the experimental range. We observe that $\eta = 1$ (no sliding) for $\theta_i < 45^\circ$ typically. For $\theta_i > 45^\circ$, η is significantly smaller than unity, which proves that the condition of nonsliding is not reached when the ball leaves the surface. The interpolation of the experimental data to Eq. (8) makes it possible to determine the critical angle $\theta_i^c = 46.2^\circ$ (vertical dashed line). The gray curves are for $\varepsilon_z = 0.9$ and $\mu = 0.22$ for the solid curve. Dashed lines, plotted for $\mu = 0.18$ and $\mu = 0.26$, underline the sensitivity to the value of the friction coefficient.

friction coefficient, $\mu \simeq 0.2$. In the next section, we analyze the behavior of the system for larger incidence angles and then further discuss the value of the friction coefficient.

D. Large incidence angle $\theta_i > \theta_i^c$

Beyond the critical angle θ_i^c, the contact point between the ball and the substrate slides throughout the contact. The angular velocity ω_r is smaller than that obtained from rolling conditions (Fig. 3) and the reflected angle θ_r is larger (Fig. 5) than expected without sliding.

Beyond θ_i^c, the relation between the changes in the normal and in the tangential velocity holds and we have $v_{y,r} - v_{y,i} = \mu(v_{z,r} - v_{z,i})$. In addition, from Eq. (2), we have $R\,\omega_r = -\frac{3}{2}\mu(v_{z,r} - v_{z,i})$. One can thus write the ratio of the final angular velocity ω_r to the final tangential velocity $v_{y,r}$ in the form

$$\frac{R\omega_r}{v_{y,r}} = \frac{\frac{3}{2}(1+\varepsilon_z)\mu}{\tan(\theta_i) - (1+\varepsilon_z)\mu}. \tag{8}$$

The interpolation of the experimental data in Fig. 6 with $\varepsilon_z = 0.9$ leads to $\mu = 0.22$ and $\theta_i^c = 46.2^\circ$. Complementary experimental data beyond 60° would be necessary to confirm that ω_r tends to 0 when the incidence angle tends to 90°. However, for practical reasons, the experimental setup does not make it possible to study angles larger than 60°. We observe in Fig. 6 that Eq. (8) does not perfectly fit the data beyond θ_i^c when ε_z is assumed to be constant. In principle, we can introduce the experimental values of ε_z in Eq. (8) which leads to a better interpolation of the data but does not provide more insights on the mechanisms at play. Thus, we consider a good agreement between the analytic model and the experimental data, even if ε_z is constant.

Finally, one can report in Fig. 5 the predicted value of $\theta_r - \theta_i$ as a function of the incidence angle θ_i. We have

$$\tan\theta_r = \frac{1}{\varepsilon_z}\tan\theta_i - \mu\frac{1+\varepsilon_z}{\varepsilon_z}. \tag{9}$$

Again, based on the aforementioned values for ε_z and μ, one observes an excellent agreement between the model and the experimental data.

IV. DISCUSSION AND CONCLUSION

We reported an experimental study of the rebound of a table-tennis ball colliding without initial spin with a rigid surface. The most striking result is that, for a large range of incidence angles and velocities, perfect rolling prevails so that the final translational and angular velocities can be predicted without any knowledge of the material or contact properties. The result is even more striking if one considers that the ball shell is in most cases subjected to a mechanical instability that leads to elastic buckling in the contact region, as we know from a previous study [10] and as documented elsewhere [12–14].

On the one hand, we observe that the introduction of an incidence angle does not affect the rebound along the normal to the substrate. Indeed, reporting the normal velocity restitution coefficient ε_z as function of the initial normal component of the velocity $v_{z,i}$, we observe that all the experimental data follow the same trend regardless of the tangential component of the velocity $v_{y,i}$ (Fig. 4). Moreover, we observe that the normal restitution coefficient exhibits two regimes as a function of the normal incident velocity $v_{z,i}$. The transition between the two regimes is due to the buckling of the spherical shell which occurs above a critical normal velocity of about 7.5 m s^{-1}, compatible with previous measurements obtained in normal incidence with the same system [10].

On the other hand, we observe that the buckling of the ball shell does not significantly alter the spin of the ball after rebound. For sufficiently small incidence angles θ_i, the collision conditions are such that the ball leaves the substrate while rolling without sliding. The reflected translational and angular velocities do not depend on the material properties. In addition, the reflected angle can be well predicted just knowing the restitution coefficient of the normal component of the velocity, acknowledging that this one might depend on the constitutive material of the ball. Beyond a critical angle of incidence the contact point between the ball and the substrate still slides when they separate. In this case, the translational and angular velocities after rebound can be predicted provided the supplementary knowledge of the friction coefficient μ.

To reinforce our conclusions, we repeated the experiment with a second type of table-tennis ball (made of celluloid) presenting significantly different experimental parameters (frictional coefficient $\mu \simeq 0.16$ and restitution coefficient $\varepsilon_z \simeq 0.84$). For the sake of clarity, the results are not shown here but the agreement is again excellent and, for instance, the measured critical angle is of about $\theta_i^c \simeq 35^\circ$ in this case, as expected from Eq. (7).

The present results represent an important step for the understanding of the rebound of the table-tennis ball on the racket and directly apply to the rebound on the table. They lead us to think that there are only a few ways to modify the ability of the racket to provide effects (spin) to the ball and that the angular velocity cannot exceed $\omega_r = \frac{3}{5} v_{y,i}/R$. We must remind here that we considered a substrate that cannot deform and load elastic energy. Indeed, the stiffness of the ball and surface materials differ so much that no elastic energy can be stored in the tangential deformation. A natural extension of the present study to the case of collision with soft and elastic surfaces (corresponding to the paddles polymeric layers) is in progress.

ACKNOWLEDGMENTS

T.R. gratefully acknowledges the GDR Sport & Activité Physique for its financial support. The authors also thank F. Vittoz for his technical help in the design of the experimental setup.

[1] H. Brody, That's how the ball bounces, Phys. Teach. **22**, 494 (1984).
[2] R. Cross, Measurements of the horizontal coefficient of restitution for a superball and a tennis ball, Am. J. Phys. **70**, 482 (2002).
[3] R. Cross, Grip-slip behavior of a bouncing ball, Am. J. Phys. **70**, 1093 (2002).
[4] W. J. Stronge and A. D. C. Ashcroft, Oblique impact of inflated balls at large deflections, Int. J. Impact Eng. **34**, 1003 (2007).
[5] N. Maw, J. Barber, and J. Fawcett, The oblique impact of elastic spheres, Wear **38**, 101 (1976).
[6] N. Maw, J. Barber, and J. Fawcett, The role of elastic tangential compliance in oblique impact, J. Lubr. Technol. **103**, 74 (1981).
[7] H. Dong and M. Moys, Experimental study of oblique impacts with initial spin, Powder Technol. **161**, 22 (2006).
[8] D. Gorham and A. Kharaz, The measurement of particle rebound characteristics, Powder Technol. **112**, 193 (2000).
[9] R. Cross, Oblique impact of a steel ball, Powder Technol. **351**, 282 (2019).
[10] T. Rémond, V. Dolique, F. Vittoz, S. Antony, R. G. Rinaldi, L. Manin, and J.-C. Géminard, Dynamical buckling of a table-tennis ball impinging normally on a rigid target: Experimental and numerical studies, Phys. Rev. E **106**, 014207 (2022).
[11] J. Schindelin, I. Arganda-Carreras, E. Frise, V. Kaynig, M. Longair, T. Pietzsch, S. Preibisch, C. Rueden, S. Saalfeld, B. Schmid *et al.*, Fiji: An open-source platform for biological-image analysis, Nat. Methods **9**, 676 (2012).
[12] M. Hubbard and W. Stronge, Bounce of hollow balls on flat surfaces, Sports Eng. **4**, 49 (2001).
[13] X.-W. Zhang and T. Yu, Experimental and numerical study on the dynamic buckling of ping-pong balls under impact loading, Int. J. Nonlinear Sci. Numer. Simul. **13**, 81 (2012).
[14] R. G. Rinaldi, L. Manin, C. Bonnard, A. Drillon, H. Lourenco, and N. Havard, Non linearity of the ball/rubber impact in table tennis: Experiments and modeling, Procedia Eng. **147**, 348 (2016).